ASPECTS FOR THE DESIGN OF GAS CAVERNS IN THE BORDER REGION OF SALT DOMES – ROCK MECHANICAL CALCULATIONS

Kurt Staudtmeister , Dirk Zapf

Institut für Unterirdisches Bauen (IUB) - Leibniz Universität Hannover
Welfengarten 1a, D 30167 Hannover, Germany

Abstract:

For several reasons the demand for storage capacity for natural gas has increased drastically during the last years. Existing gas cavern fields have been extended and new storage locations have been explored. In order to obtain a high degree of exploitation there is a need for creating caverns close to the boundaries of the salt formations.

For the design of such caverns it is important to get sufficient knowledge of the geometry of the interface between rock salt and caprock as well as the initial conditions with respect to rock mass stresses and rock mass temperatures. Within the rock mechanical calculations these assumptions are crucial for the determination of sufficient spacing without influencing the stability or the tightness of the storage cavity.

The paper describes by the way of example the situation for a salt dome cavern configuration. By three-dimensional calculation models the rock mechanical design is shown. Special focus is set on the criteria for the assessment of stability and tightness of the caverns in the boundary region of the salt formation.

Keywords:rock mechanics, structure of salt domes, numerical analysis

1 Background

In the design of new caverns it is sufficient to use axisymmetric models for the numerical calculations of caverns in rock salt. Especially when the distance to the boundary of the salt dome and to a neighbour cavern is sufficiently high, the model can designed as an axisymmetric model with relatively small dimensions. In several cases this simplification cannot be accepted when these assumptions are not conservative enough or lead to economical less favourable recommendations.

Finite Elements calculations with models of salt domes and caverns are carried out since several years /4/. Due to the development of faster computer systems and more powerful 3D- analysis programs, it is possible to calculate large models with complex and irregular shaped cavern geometries today /6/. Calculations with a large calculation model considering two caverns in different depths and different loading conditions have been carried out /1/.

During the last years the extensive enlargements of gas storage capacity lead to the construction of new caverns within existing cavern fields. Due to limited space in the salt structure or for obtaining high working gas volumes the configurations partially deviate significantly from axi-symmetric situations. The reasons are

- location at the boundary of the salt dome (sloping flanks),
- deeper caverns in the vicinity of existing caverns at shallower depth,
- geological situations with relevant non-halite layers.

The basic information about the structure of the salt deposit and the decision about cavern locations is based on geological 3D- modeling /9/. Relevant characteristics from the geological model have to be taken into account within the geomechanical model.

There are many well documented common salt domes all over the world, considerable are e.g. the gulf of Mexico /11/ and /14/, the southern north sea region /2/ and /7/ or the salt domes in the Zagros Mountains in Iran where the salt domes came up to the surface /8/.

The age of a salt dome can be numbered with several millions of years. An overview of the development of salt domes is given in several literatures e.g. /5/ /10/ /21/ /22/. The dimension and the velocity of a salt dome are depended on the geological structure of the non-halite rock mass surrounding the salt dome.

Three stadiums are describing the vertical movement or halokinesis of a salt dome. In a first stadium there is a development of small cambers at the salt surface. These are formed e.g. as salt pillows or salt swells. Because of the differential pressure due to growth faults in the non-halite top layers the growth rate of the salt diapir increases. In the second stadium the salt domes are breaking upwards through the top layers while the salt dome surrounding rock masses are moving downwards. The third stadium describes a horizontal dispersion of the salt dome with a typical mushroom-shaped form. This development of the salt dome can only take place if there is still a trunk to the original salt layer which supplies the dome with more salt.

Investigations of the shape of a salt dome are always in the focus of interest /3/, /9/ and /13/. Detailed information of the edge of salt is important for the solution of a cavern in a location near the boundary of the salt dome /12/ for an economical and save operation of a cavern. For this reason it is important to get knowledge of the initial stress state in a salt dome, especially with a focus on the boundary region. Calculations regarding these questions had been carried out /16/. The model calculations carried out there showed that the assumption of an isotropic stress field within the rock salt formation is valid (figure 1).

This paper shows the calculations of the stress states in a salt dome and reviews the conditions especially at the boundary region of the salt.

2 Assessment of the Initial Conditions

Within the paper the focus is set on the stress state interaction between the assumed cavern and the boundary of the salt dome. The modeling phase is structured in

- the initialization of the lithostatic stress,

- the creep calculation of the model over a period of 10,000 years and
- the investigation of feasible maximum and minimum pressures for the different cavern models dependent of the distance between the cavern and the salt dome boundary.

The initial stress is an important value for the recommendations from the rock mechanical point of view. The assessment of the predicted model conditions in the vicinity of the storage caverns has to be based on design criteria with adequate measures which define levels of safety. The main objective here is not to introduce a specific project but to explain possible procedures within the rock mechanical design.

2.1 Theoretical Calculation Models

The theoretical models has to take into account the site specific in situ and operating conditions of the rock mass around the cavern and the cavern itself in terms of the

- initial state of stress and rock mass temperature,
- distance between the cavern and the boundary of the salt dome,
- material behavior of the salt and the non-halite rock masses,
- density assumptions of the rock formation,
- horizontal and vertical extend of the rock mass and
- the loading histories i.e. the internal pressure versus time.

Figure 2 shows the geometrical situation of example calculation for a cavern near the salt dome boundary. The model is a section of the salt dome model from /16/ as shown in figure 3. It has a height of 1,080 m in z-direction and a width of 950 m in x-direction respectively 400 m in y-direction. The top of the calculation model is in a depth from top ground surface of 500 m, the bottom is in a depth of 1580 m. The non-halite surrounding rock mass comprises a layer of chalk with a thickness of 220 to 370 m and a layer of sandstone with a thickness of 710 m. A risen salt dome often contains a layer of caprock on the top of the salt dome /15/ /20/. In the calculation model a 30 m thick caprock layer is considered above the rock salt mass. The cavern itself has a height of 300 m and a diameter of 80 m. Also distinguishable in this figure is the vertical section A-A and the horizontal section B-B for later analysis. The smallest distance "a" between the cavern and the salt dome boundary is approximately 180 m in this calculation model 1 (CM 1).

In order to investigate the influence of the spacing between the cavern and the boundary of the salt dome two further calculation models has been created (CM 2 and CM 3). They have a lower distance "a" from the cavern to the salt dome border of 130 m respectively 90 m in horizontal direction. For a better comparison of the three calculation models the depth of the cavern has the same value in every model. The assumptions for the geology, constitutive laws, parameters and primary stress states are the same in every calculation model.

The initial state of stress and temperature has been taken in a reasonable order of magnitude and of course has to be calibrated when performing a site-specific design. The densities are assumed as follows:

- Rock Salt = 2.20 t/m^3
- Quarternary = 2.08 t/m^3
- Chalk = 2.08 t/m^3
- Sandstone = 2.60 t/m^3
- Caprock = 2.60 t/m^3.

The initial temperature distribution is:

- T = 286 K at the surface
- Gradient with depth T' = 0.0317 K/m.

The assumptions mentioned above lead to a rock mass temperature of 301 K (28°C) at the top of the model and a temperature of 336 K (62°C) at the bottom of the calculation model at a depth of 1,580 m. Figure 4 shows the temperature distribution in the model. Of course the influence of the temperature is only considered in the creep behavior of the rock salt mass.

The initial state of stress is calculated assuming isotropic conditions in the rock salt mass i.e. the lateral pressure coefficient is set to $K_0 = 1$, the non-halite surrounding rock mass is set to $K_0 = 0.5$.

The material parameters of the salt rock are determined for the LUBBY2 material law on the basis of laboratory tests showing an average rock salt behavior /18/. For the calculations the software Flac^{3D} is used. The constitutive law for the non-halite rock mass is the elastic formulation by HOOKE. For the first assumption, the young's modulus for the specific rock formations is set as followed:

- Rock Salt E = 21,550 MPa
- Chalk E = 1,000 MPa
- Sandstone = 10,000 MPa
- Caprock E = 10,000 MPa.

The calculation is divided into the following phases:

- In a first step the lithostatic pressure is initialized into the model with the above mentioned assumptions of the densities and the lateral pressure coefficient (figure 5).
- The second step contains the elastic calculation to bring the model into a state of equilibrium.
- After reaching a stable equilibrium state the creep calculations with the creep law LUBBY2 is getting started with an overall calculation time of 10,000 years to reach an equilibrium state in the rock salt mass.

The operating history has been set as follows:

- Phase A: Internal pressure of 20.0 MPa for the cavern representing a range of respective maximum pressures for a computation time of 730 days.
- Phase B, Case 1: Internal pressure decrease to a level of 3.0 MPa within 14 days and remains under this pressure for a longer period for an investigation of a feasible minimum pressure.
- Phase B, Case 2: Internal pressure decrease to a level of 5.0 MPa within 14 days
- Phase C: After 90 days the cavern is repressurized to maximum pressure range.

2.2 Rock Mechanical Calculations

The rock mechanical calculations are performed using the Flac^{3D} software from Itasca applying the material law LUBBY2 for the material behavior of rock salt via the user-defined-model interface of the software simulated. The non-halite layers are calculated with the elastic formulation of HOOKE. Figure 6 and 7 show the 3D-FD-Model. Overall the model has 42,700 zones and 47,046 grid-points.
The first simulation with the CM 1 is carried out with the above mentioned conditions. In further calculations the different distances between the cavern and the salt dome boundary are going to be calculated.

3 Assessment of the Calculation Results

Focusing on the recommendation of a minimum and a maximum internal pressure the state variables in terms of principal stresses are evaluated as described in the following chapter.

3.1 Minimum Pressure

The assessment of the states of stress in the rock mass in the vicinity of the cavern is carried out applying the stress intensity index . This index is calculated on the basis of the results of the numerical calculations /19/. Among other criteria the value of the stress intensity index is a measure for the determination of the permitted minimum pressure and corresponding durations under this pressure for the gas caverns during operation.
This procedure leads to a dimensioning which excludes any spalling of a part of the cavern periphery. The stress intensity index indicates the percentage actually used of the potential stress which the rock mass could absorb during short term stressing. It is defined by

$$\eta = \frac{\sqrt{2 \cdot J_2^D}}{\beta(\sigma_{iso})} \qquad (1)$$

where $\sqrt{2 \cdot J_2^D}$ is the existing deviatoric stress and $\beta(\sigma_{iso})$ is the fracture strength under short term loading for the given states of stress. J_2^D is the second invariant of the stress deviator tensor.

$$J_2^D = \frac{1}{6}\left[(\sigma_1 - \sigma_2)^2 + (\sigma_2 - \sigma_3)^2 + (\sigma_1 - \sigma_3)^2\right] \qquad (2)$$

$$\sigma_{iso} = (\sigma_1 + \sigma_2 + \sigma_3)/\sqrt{3} \qquad (3)$$

The fracture strength $\beta(\sigma_{iso})$ is obtained from uniaxial and triaxial laboratory tests /18/. Figure 8 is a schematic explanation of the $\beta(\sigma_{iso})$ strength which is determined separately for the stress states of triaxial compression and triaxial extension.

Application for Calculation Models CM1, CM2 and CM 3

Figure 9 shows the development of the rock mass stressing for different points in time for the calculation model 1 with the largest distance between the cavern and the salt dome boundary. Phase A at high internal pressures results in low values for the stress intensity index. During phase B of gas withdrawal the stressing concentrates at the cavern periphery. The degree of stressing (-level) at the end of this phase here at t = 744 d highly depends on the pressure decrease rates. For this stress concentration at the cavern walls the interaction with the salt dome boundary is of minor importance. The time period of phase B for a certain time is characterized by stress redistributions leading to an increase of the stress intensity index in larger rock mass regions in the surroundings of the caverns. Here interference is likely to take place if the cavern is situated closer to the salt dome border.

Consequently the interaction of the cavern and the salt dome border for calculation model CM 1 is low, the results of the stress intensity index around the cavern shows a nearly symmetric distribution until 774 d. Only the last shown point in time (834 d) shows a moderate interaction and asymmetric distribution between the cavern and the salt dome border. The results of this calculation are also shown in a horizontal cross section B-B in figure 10.

A more obvious interaction shows the result for calculation model CM 2 (figures 11 and 12). The stress intensity index is now already influenced at 774 d. In the further calculation, the asymmetric distribution is getting concentrated between the cavern and the salt dome border.

CM 3 is the calculation model with the lowest distance from the cavern and the salt dome boundary. Figure 13 shows that the 20 % zone fills large parts of the rock salt region between the border and the cavern after 834 d. This asymmetric distribution is also visible in the stress intensity index in figure 14 along the horizontal cross section B-B.

From an engineering point of view and taking a safety factor into account a cavern has to be adequate far away from the salt dome boundary. Local zones of weakness may occur and especially a transition zone at the salt dome boundary with inhomogeneous salt regions may occur. These lead to a further increase of the stress concentration in the focusing rock salt region. It has to be remarked that only an extremely small amount of rock salt material can be tested in the laboratory. Whether the results are representative for the whole rock mass around the caverns with respect to strength properties only can be checked by carefully evaluated sonar measurements during the operation phase of the caverns.

In order to avoid the consequences of uncertainties a gas cavern should be located with a distance large enough to guaranty the stability and integrity of the cavern wall.

3.2 Maximum Pressure

The safety at maximum pressure level means that the integrity of the rock mass surrounding cavern has to be guaranteed. No macroscopic fracture should be initiated at this pressure level in the surrounding rock mass. Therefore it is generally accepted that tensile stresses in the region around the storage caverns have to be avoided.

In addition considering aspects of serviceability or usability of the cavern the surrounding rock mass has to be tight, not only in a technical sense but also by means of infiltration of small gas volumes into the rock mass. Additionally in the case considered here no connection between the caverns should exist in order to assure a safe and independent operation of the individual caverns.

The applied safety assessment has been investigated in detail in /17/. The basic ideas of this criterion can be described briefly as follows:

- An ongoing permeation of gas into the surrounding rock salt mass can be excluded if a continuous so called 'safety zone' is spreading around the cavern, where the values of the effective tangential stresses $_{teff}$ remain below a boundary value $_{teff}^{*}$. Bearing in mind that compressive stresses are negative by definition, this means, that the compressive stresses acting perpendicular to the direction of infiltration have to be higher in level by a certain amount than the internal cavern pressure.
- At the same time this specific safety zone has to show a minimum extent a^{*}.
- The limiting value $_{teff}^{*}$ for the stress difference in the zone and the absolute extent a^{*} are resulting from safety considerations.
- Taking these two parameters – effective tangential stress $_{teff}$ and the extent of the zone a – as design variables the influence of the different cavern model parameters, for example the shape of the cavern roof, on the safety at maximum pressure state can be shown quantitatively.

The adopted evaluation criterion is summarized in Figure 15.

Application for Calculation Models CM1, CM2 and CM 3

As example the internal pressure in the cavern is increased to 19.0 and 20.0 MPa respectively for each calculation model. For all these studies the individual principal stresses remain in the compressive region under these internal pressures.

Figures 16 to 18 show the stress difference between $_2$ and P_i or devolved the spread of the safety zones under maximum pressure conditions around the cavern. For each calculation model it is visible that the distance to the salt dome border has an influence on the distribution of the safety zone which is asymmetric in each case. This can also be observed in the results of calculations with to caverns at different depths /1/. The thickness of this safety zone is not significantly depending on the distance to salt border. It can be assumed that the spread of the safety zone becomes more symmetric if the cavern has a larger distance from the salt dome boundary.

In order to a possible transition zone occurring at the salt dome boundary it is necessary to have a distance large enough between the cavern and the salt dome boundary from an engineering point of view.

4 Conclusions

Because the transition to non-isotropic initial stresses in the neighboured rock mass occurs in the non-halite layers the assumption of an isotropic initial stress field in the rock salt formation is likely to be valid in most cases.

The paper shows the suitability of using the rock salt mass for the creation of storage caverns even in the boundary region of salt domes without changing the generally applied lateral pressure coefficient of $K_0=1$. However within a robust design for the layout of caverns sufficiently high distances to the border of the halite formation have to be recommended in order to avoid significant stress redistributions in the zone below top of salt or flanks. The exact distances, the location

of the salt/non-salt interface and possible extensions of local weakness zones only can be assessed by the geological description of the salt dome boundary.
If a precise description is missing sufficient distances only can be determined by an engineering assessment. For gas caverns the demand of a sufficiently extended safety zone ensuring the tightness of the system has to be proven. All the significant stress redistribution zones and the safety zone with respect to tightness have to be located in homogeneous rock salt mass. Transition zones with higher permeabilities and stiffness contrasts compared to the rock salt properties should not be used for load bearing purposes. Additional safety distances have to be provided for special load cases like unintentional pressure drops.

References

/1/ Achmus, M., Rokahr, R., Staudtmeister, K. and Zapf, D.;
Rock Mechanical Aspects of Gas Cavern Interaction for non-axisymmetric Conditions; Technical Paper, SMRI Fall Meeting, Austin, Texas, USA, October 13-14, 2008.

/2/ Arndt, S., Götze, H.-J., Hese, F., Rabbel, A., Schlesinger, A. and Theilen, Fr.;
Salt diapir evolution in the German North Sea sector; Geophysical Research Abstracts, Vol. 8, 06166, 2006.

/3/ Blair, R. and Keeter, J.;
Case History – Using Horizontal Drilling to Determine the Edge of a Gulf Coast Dome; Technical Paper, SMRI Fall Meeting, Rome, Italy, 4-7 October 1998.

/4/ Dwyer, M. and Thoms, R.;
Finite Element Analysis of Salt Domes with Stored Hot Wastes; Fourth International Symposium on Salt – Northern Ohio Geological Society, 1974.

/5/ Eisbacher, G.,
Einführung in die Tektonik; Enke Verlag Stuttgart, 1996.

/6/ Riekenberg, R., Hartmann, U., Staudtmeister, K. and Zander-Schiebenhöfer, D.;
Recommendation of Maximum Cavern Pressures for the Gas Storage Caverns at Huntorf on the Basis of Three-Dimensional Numerical Models; Technical Paper, SMRI Fall Meeting, Berlin, Germany, October 3-6, 2004.

/7/ Jacobsen, L.J. and Nielsen, B.L.;
Structural Studies of a Danish Salt Dome Optimize Construction of Six Gas Storage Caverns; Seventh Symposium on Salt, Vol. 1 (151-158), 1993.

/8/ Jahani, S., Callot, J.-P., Frizon de Lamotte, D., Letouzey, J. and Leturny, P.;
The Salt Diapirs of the Eastern Fars Province (Zagros, Iran): A Brief Outline of their Past and Present; Chapter 15 in "Thrust Belts and Foreland Basins", 2007.

/9/ Kleinefeld, B., Behlau, J. and Schweinsberg, H.-J.;
Safe and Economic Cavern Construction in the Etzel Cavern Field based on Geological 3D-Modelling; Technical Paper, SMRI Spring Meeting, Porto, Portugal, April 28 - 29, 2008.

/10/ Kukla, P., Holland, M., Mohr, M., Schleder, J., Schoenherr, J. and Urai, L.;
Fortschritte bei der Integration von strukturellen, sedimatären und analogen Simulationstechnik in der Erdöl-Geologie;
DGMK-Frühjahrstagung, Celle, Germany, 2005.

/11/ Kupfer, D.,
Structure of Salt in Gulf Coast Domes; First Symposium on Salt, Cleveland, USA, 1962.

/12/ Looff, Ku., Duffield, J. and Looff, Ka;
Edge of Salt Definition for Salt Domes and Other Deformed Salt Structures – Geologic and Geophysical Considerations; Technical Paper, SMRI Spring

Meeting, Houston, Texas, USA, 2003.

/13/ Rautman, C. and Looff, Ka.;
Rapid Characterization of Salt Domes for Underground Storage; Technical Paper, SMRI Fall Meeting, Rapid City, South Dakota, USA, 1-4 October 2006.

/14/ Rautman, C., Looff, Ka., Stein, J. and Snider, A.;
An Updated Three-Dimensional Geologic-Genetic Model of the Big Hill Salt Dome and Strategic Petroleum Reserve Site; Technical Paper, SMRI Spring Meeting, Syracuse, New York, USA, 17-20 April 2005.

/15/ Martinez, J.;
Salt Dome Caprock – A Record of Geological Process; Fifth International Symposium on Salt – Northern Ohio Geological Society, 1978.

/16/ Staudtmeister, K. and Zapf, D.;
Aspects for the Design of Gas Caverns in the Border Region of Salt Domes – Initial Conditions and Assumptions; Technical Paper, SMRI Spring Meeting, Krakow, Poland, 26-29 April 2009

/17/ Rokahr, R.B., Staudtmeister, K. and Zander- Schiebenhöfer, D.;
Development of a New Criterion for the Determination of the Maximum Permissible Internal Pressure for Gas Storage Caverns in Rock Salt;
Final Report of SMRI Research Project No. 97-0001-SMRI, 1997.

/18/ Staudtmeister, K. and Rokahr, R.B.;
Laboratory Tests within the Scope of Rock Mechanical Investigations for the Design of Solution Mined Caverns in Rock Salt Mass; Meeting Paper, SMRI Fall Meeting, Hannover, Germany, Sep 25- Oct 1, 1994.

/19/ Staudtmeister, K. and Struck, D.;
Design Criteria for Prevention of Creep Rupture for Gas Caverns in Salt Rock Mass; Technical Paper, SMRI Fall Meeting, Paris, France, 1990.

/20/ Sattler, A., Rautman, C., Ehgartner, B., McHenry, J., Osbourne, G., Myers, R., Pauling, G., and Looff, Ka.;
Concerns about Sulfur Deposits in Caprock Overlying Salt Domes; Technical Paper, SMRI Spring Meeting, Syracuse, New York, USA, 17-20 April 2005.

/21/ Warren, J.,
Evaporites: Sediments, Resources and Hydrocarbons; Springer Verlag 2006.

/22/ White, R. and Spiers, C.;
Characterization of Salt Domes for Storage and Waste Disposal; Sixth International Symposium on Salt, 1983.

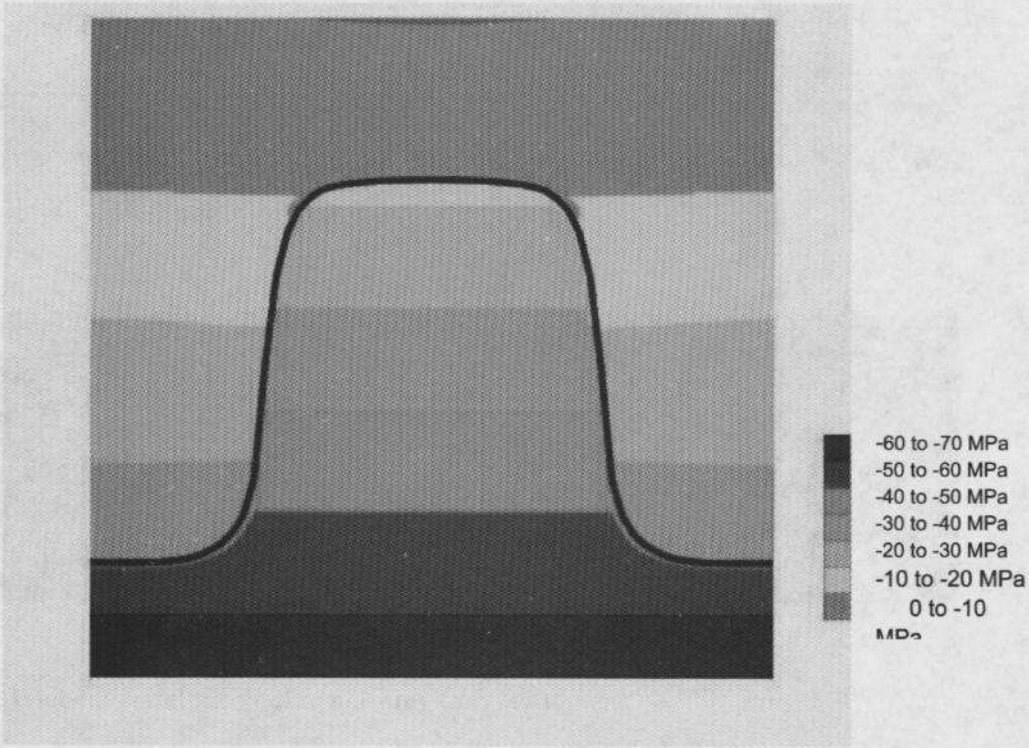

Figure 1 **Calculated stress state for a salt dome model /16/**

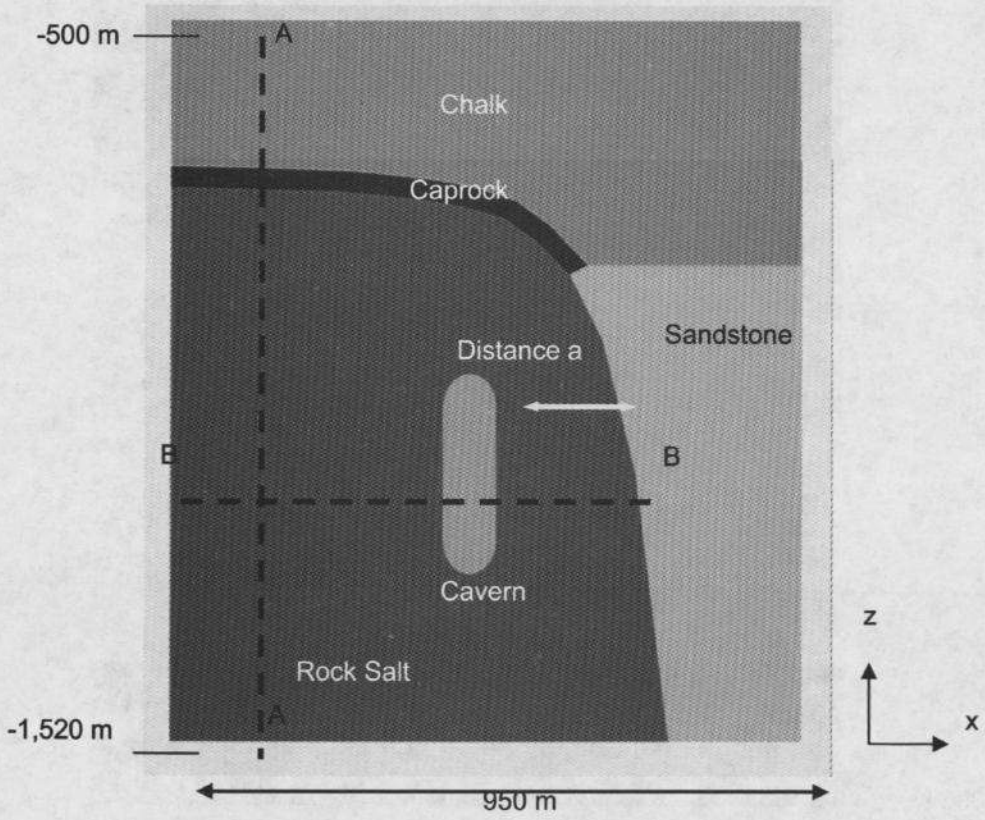

Figure 2 **Geometrical configuration of the calculation model**

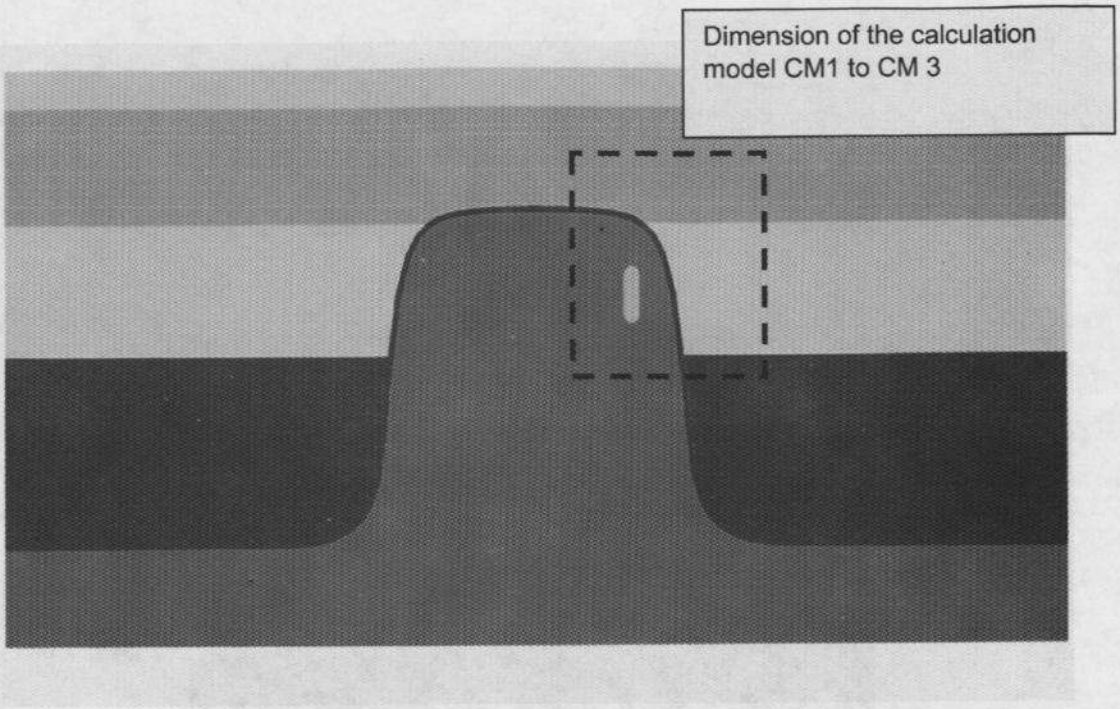

Figure 3 **Geometrical configuration of the calculation model /16/**

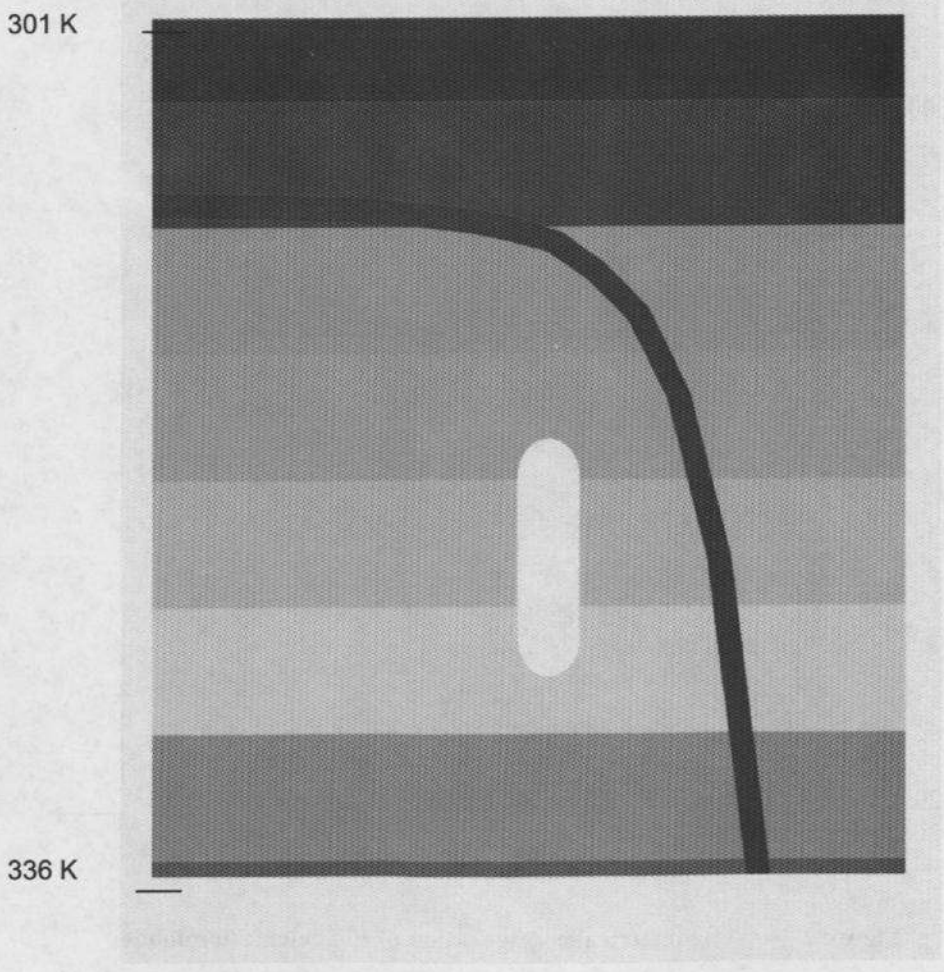

Figure 4 **Calculation model with initial state of temperatures**

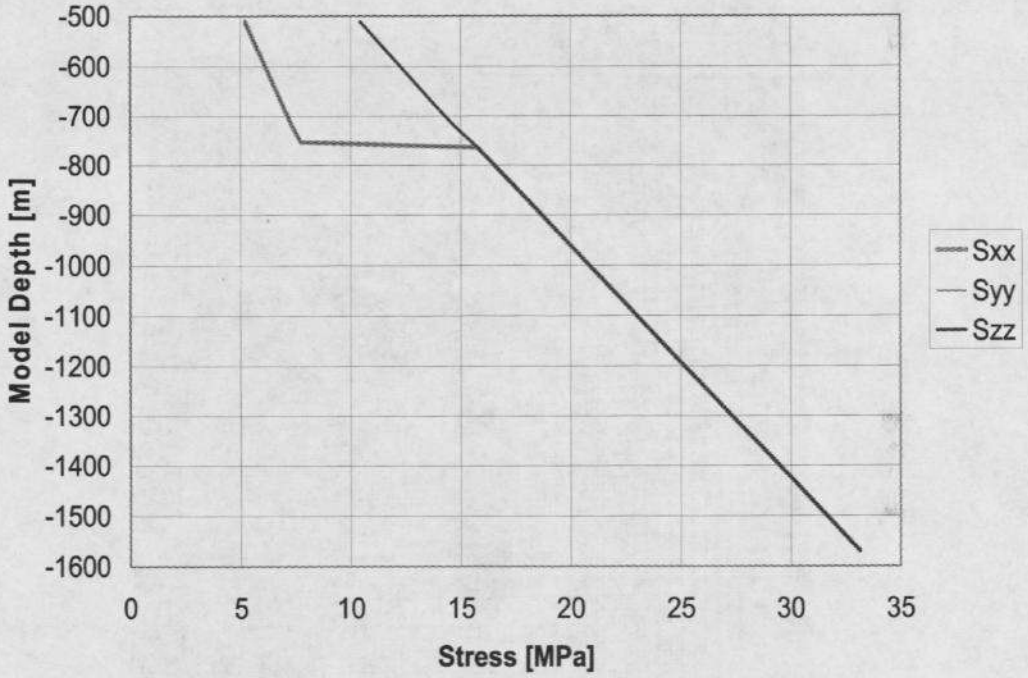

Figure 5 **Initial state of stresses in vertical cross section A-A**

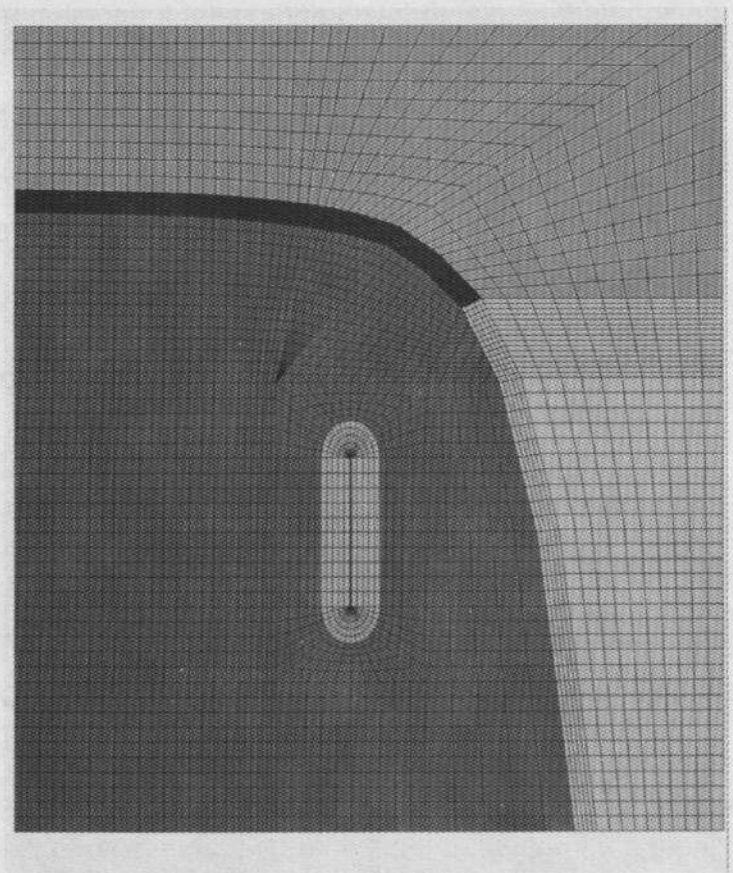

Figure 6 **Calculation model with grid**

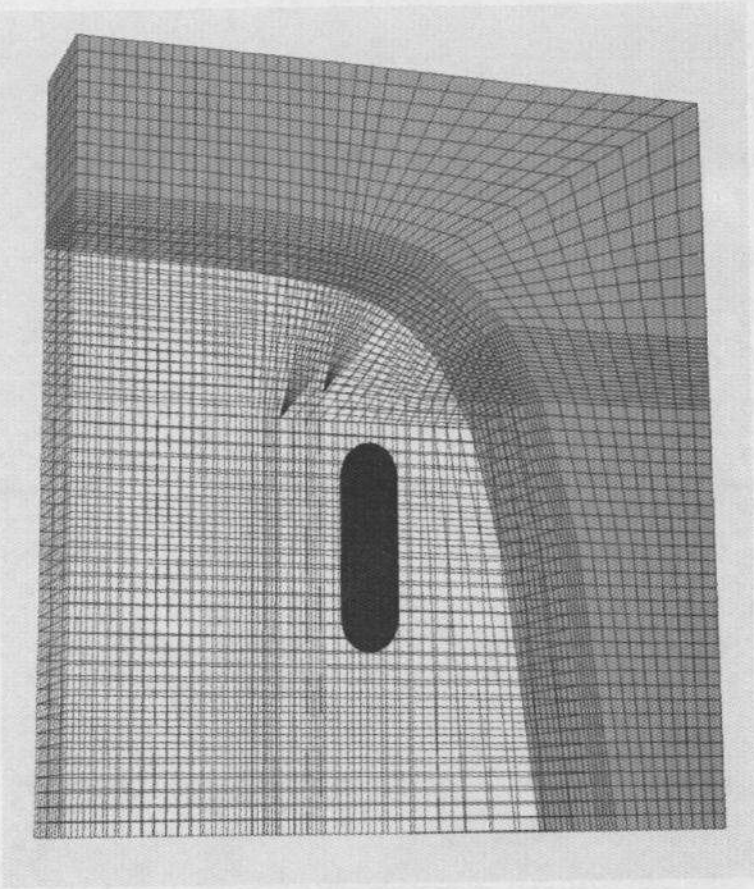

Figure 7 **3D view of the Calculation model**

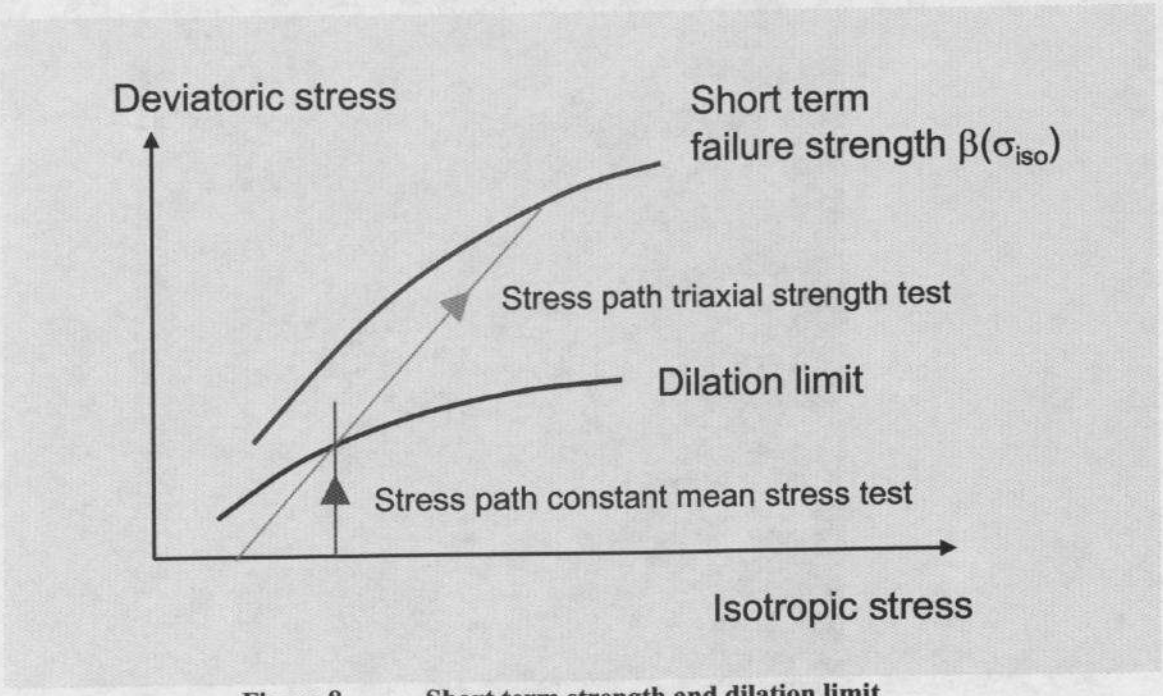

Figure 8 **Short term strength and dilation limit**

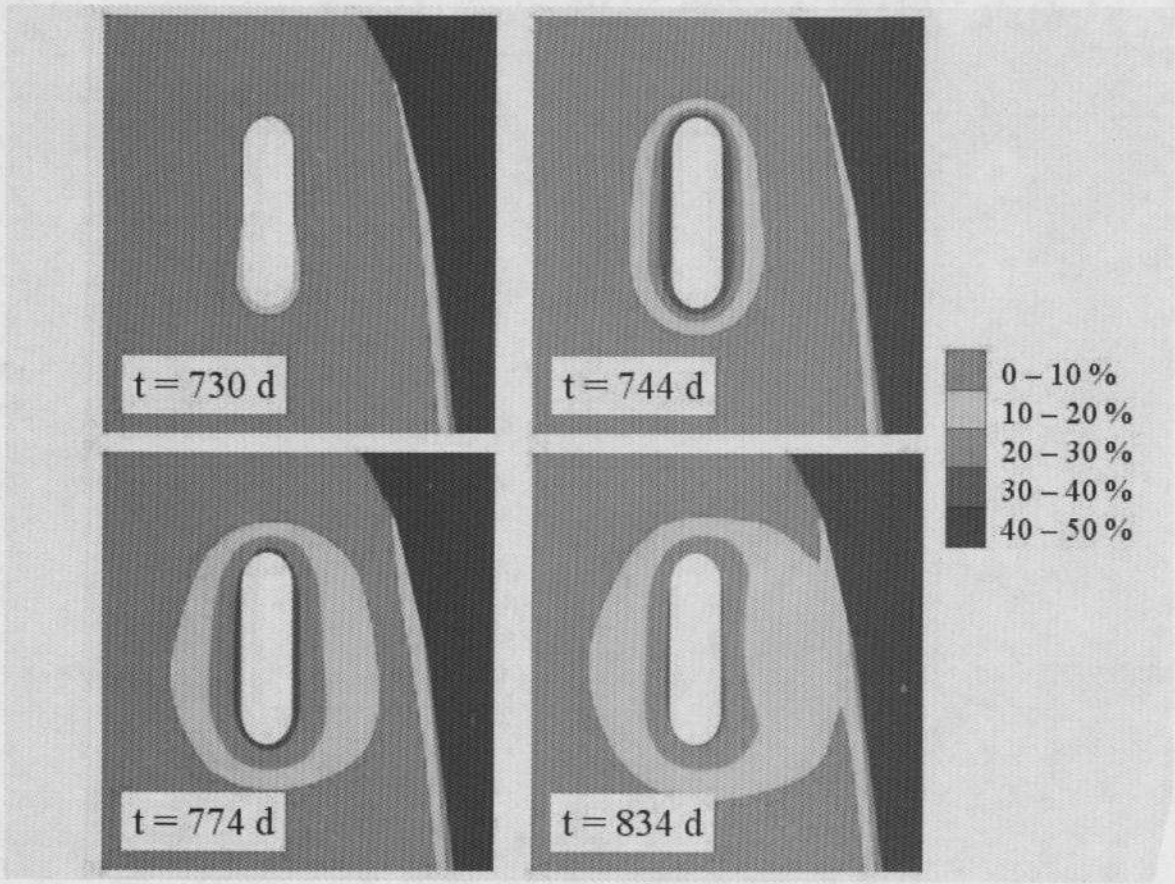

Figure 9 **Stress intensity index for calculation model CM 1**

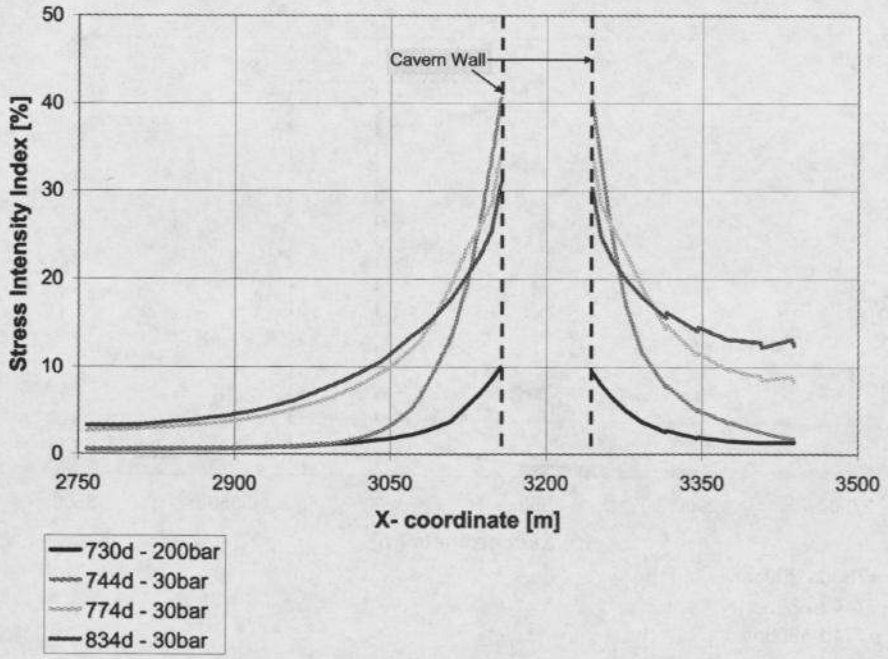

Figure 10 **Stress intensity index for calculation model CM 1 in B-B**

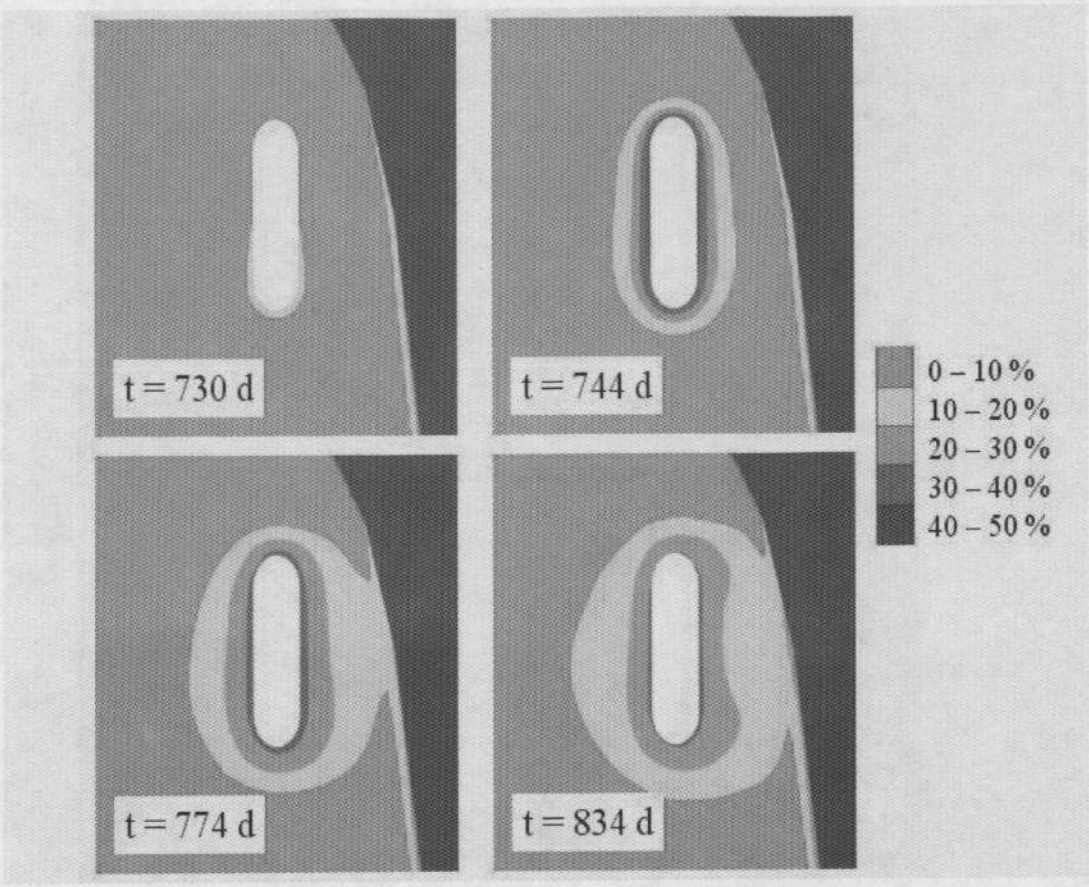

Figure 11 **Stress intensity index for calculation model CM 2**

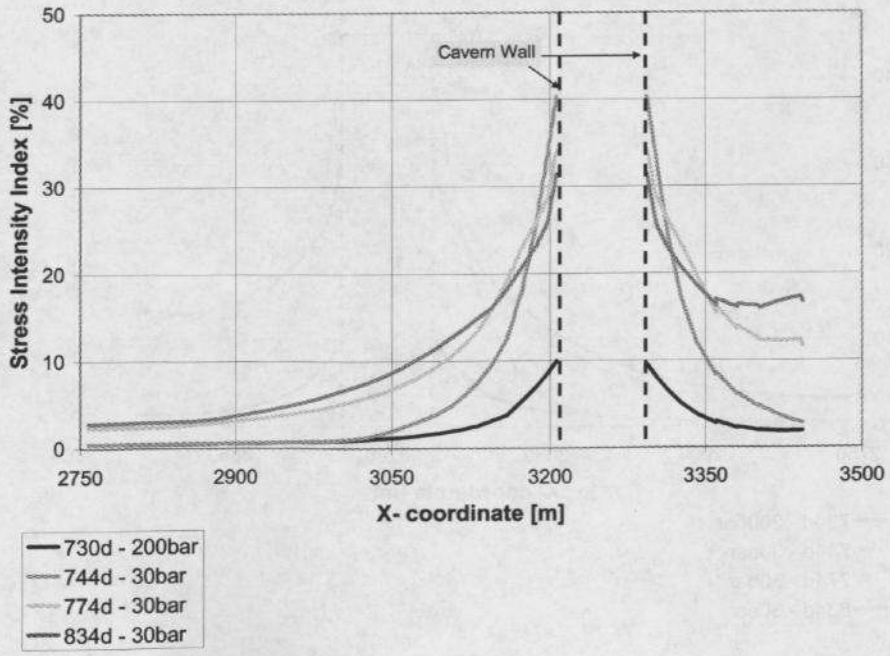

Figure 12 **Stress intensity index for calculation model CM 2 in B-B**

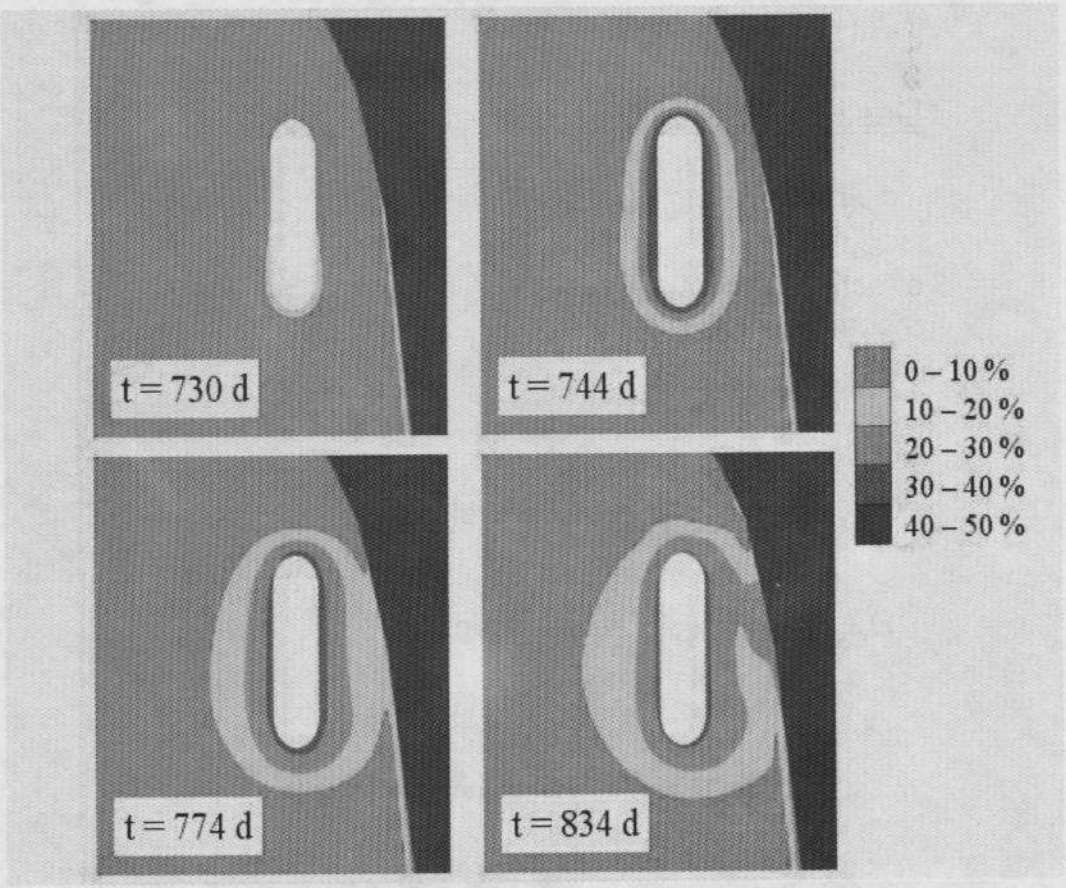

Figure 13 **Stress intensity index for calculation model CM 3**

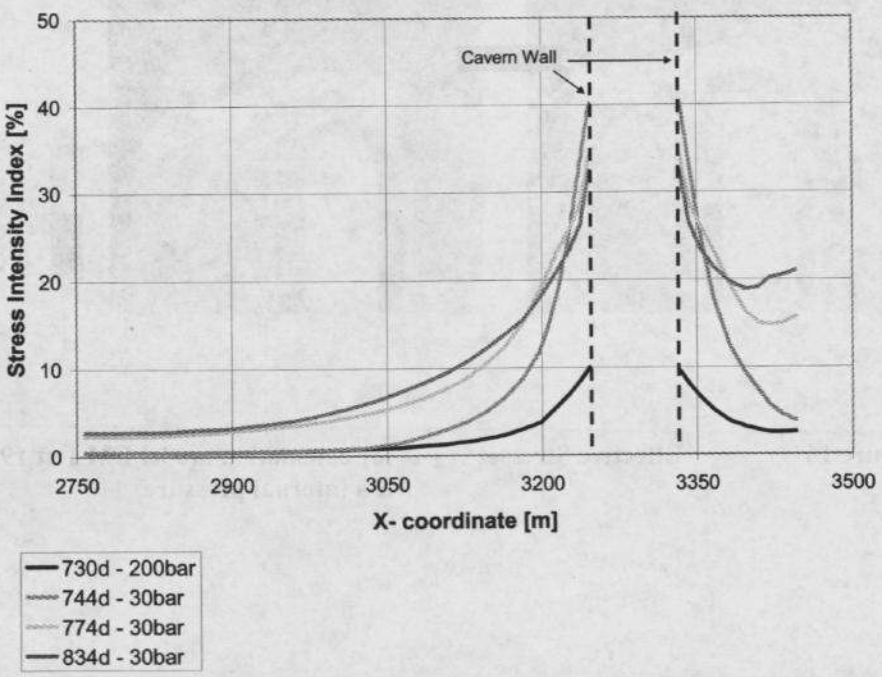

Figure 14 **Stress intensity index for calculation model CM 3 in B-B**

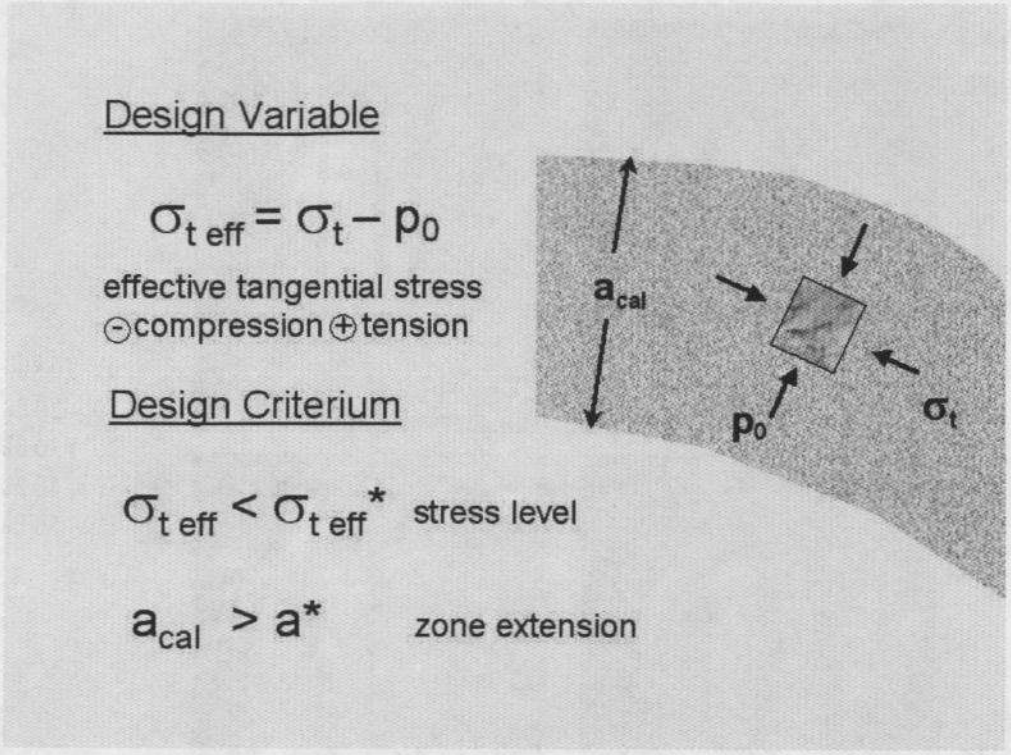

Figure 15 **Maximum pressure criterion**

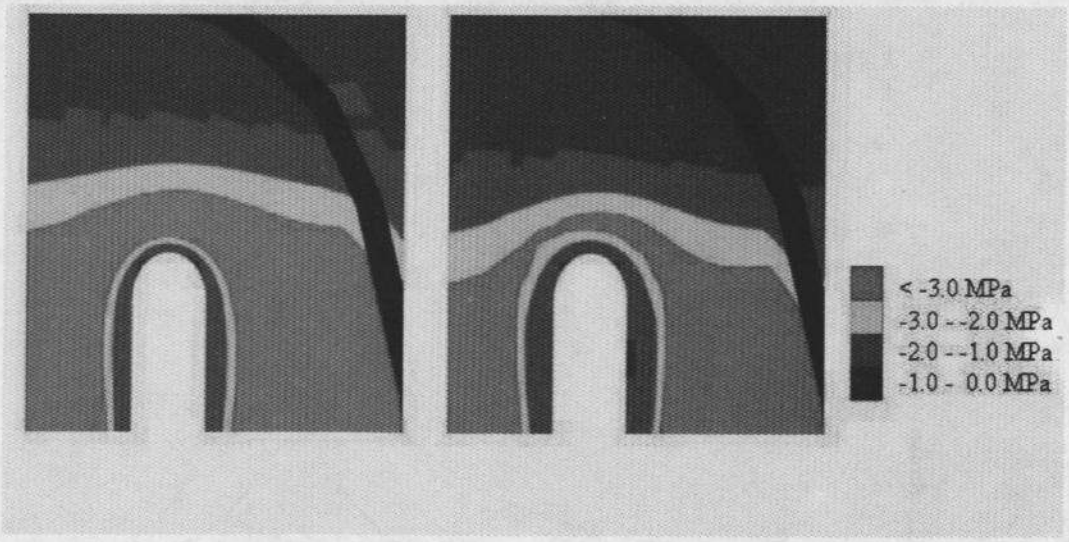

Figure 16 **Effective Stresses $_2$-P_i for calculation model CM 1 at 19.0 and 20.0 MPa internal pressure**

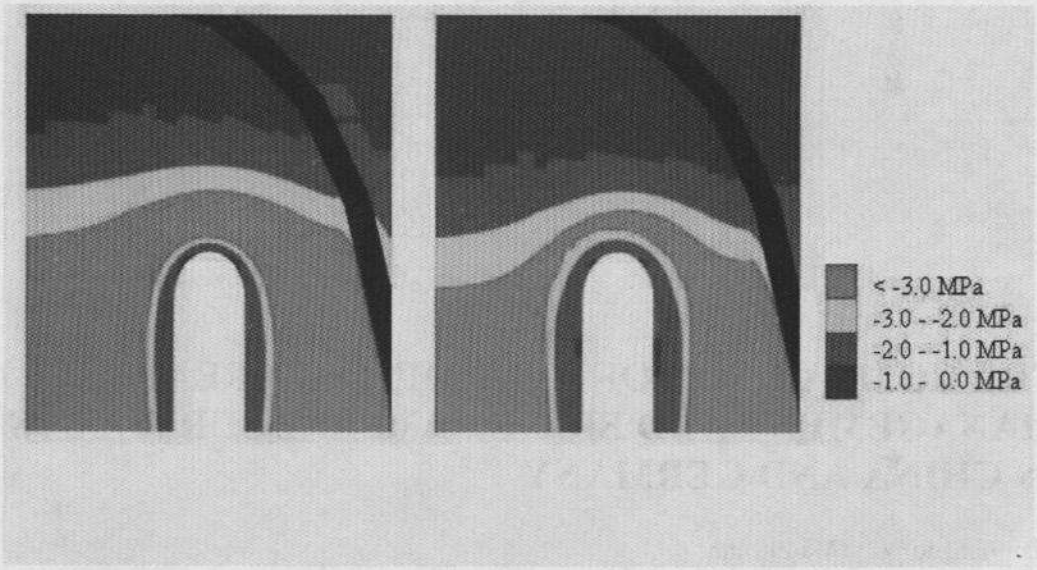

Figure 17 **Effective Stresses $_2$-P_i for calculation model CM 2 at 19.0 and 20.0 MPa internal pressure**

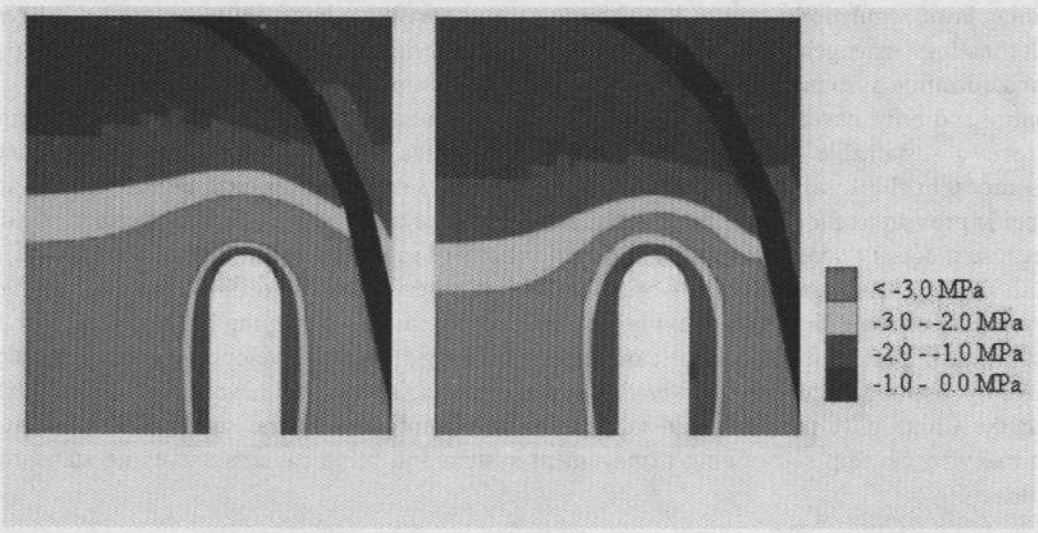

Figure 18 **Effective Stresses $_2$-P_i for calculation model CM 3 at 19.0 and 20.0 MPa internal pressure**